Multi-Mode Plasma Response and Experimental Validation

by

Z.R. Wang[1],

with N.C. Logan[1], Y.Q. Liu[2],

S. Munaretto[2], Y.W. Sun[3], J.-K. Park[1], S. Gu[3], J.M. Hanson[4],

Q.M. Hu[1], T. Strait[2], and J.E. Menard[1]

[1] Princeton Plasma Physics Laboratory

[2] General Atomics

[3] ASIPP, China

[4] Columbia University

Presented at the

60th Annual APS Meeting

Division of Plasma Physics

Portland, Oregon

November 5–9, 2018

Understanding and Identifying Each Individual Eigenmode (Stability + Mode Structure) in Multi-Mode Plasma Response is Important for Tokamak Operation

- **Tokamak plasmas sensitively respond to non-axisymmetric (3D) magnetic fields**
  - Plasma response → magnetic perturbation, plasma displacement, perturbed plasma current etc.
  - Linear theory: plasma response generally contributed by multiple stable MHD eigenmodes → multi-mode plasma response

- **Behavior of stable modes in multi-mode plasma response can significantly affect performance of tokamak operations e.g.**
  - Amplification of edge – peeling response strongly couple to edge localized modes (**ELMs**) control [Y.Q. Liu NF 2011, C. Paz-Soldan et al, PRL 2015, J.-K. Park et al, Nature Physics 2018]
  - Selective amplification of core/edge dominant modes → control of plasma rotation through neoclassical toroidal viscosity (**NTV**) [W. Zhu et al, PRL 2006]
  - Detect marginally stable modes → predict and control MHD instabilities (much of previous work based on single mode approach) [Reimerdes et al, PRL 2004]

Understanding and Identifying Each Individual Eigenmode (Stability + Mode Structure) in Multi-Mode Plasma Response is Important for Tokamak Operation

- **Multi-mode plasma response has been qualitatively identified in DIII-D and EAST experiments.**

C. Paz-Soldan et al, PRL 2015
N. Logan et al, Nucl. Fusion 2018

DIII-D n=1 plasma response

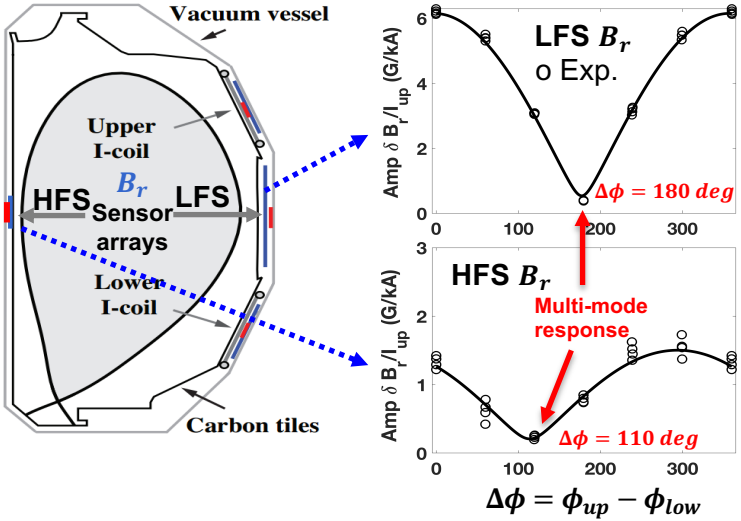

How many dominant modes contribute to multi-mode plasma response?

How about stability and behavior of dominant modes in multi-mode plasma response?

Multi-pole transfer function model is developed to reveal characters of stable dominant modes.

DIII-D NATIONAL FUSION FACILITY

Multi-Pole Response Transfer Function is Developed to Extract Stable MHD Eigenmodes from Plasma Response

Multi-pole transfer function on 3D magnetic sensor measurement is **systematically developed from generalized linear-MHD equation**:

Represent dominant eigenmodes

Measured response at jth 3D sensor

$$P_j(f,\Delta\phi) = \frac{\delta B}{I_{up}} = \sum_{i=1}^{N} \frac{a_i^j + b_i^j e^{-i\Delta\phi}(I_{low}/I_{up})}{i2\pi f - \gamma_i} + c^j + d^j e^{-i\Delta\phi}(I_{low}/I_{up})$$

f: coil frequency

$\Delta\phi = \phi_{low} - \phi_{up}$

Coupling between coil and mode at jth sensor

Eigenvalue of ith mode
Same at any sensor
Re(γ) stability index
Im(γ) mode frequency

Residual of vacuum response when $|f| \to \infty$

DIII-D n=1 plasma response

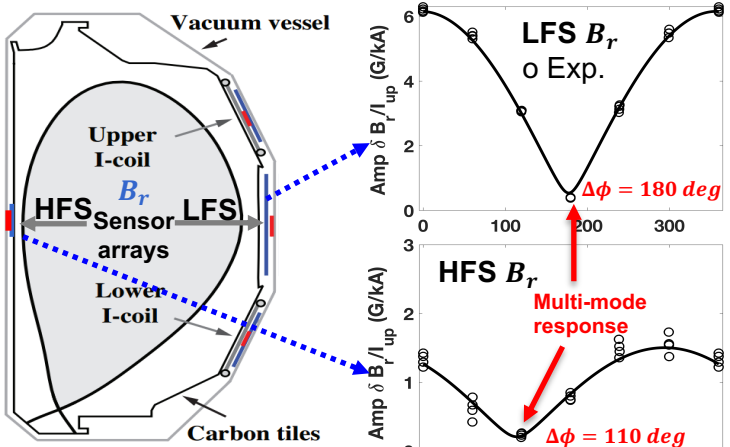

- **Combined 3D MHD spectroscopy** uses 3D coils to perform active detection (**scan f and $\Delta\phi$**) to extract transfer function and stable eigenmodes
  - Conventional passive spectroscopy detects unstable mode

Multi-Pole Response Transfer Function Extracted from Experimental Data Reveals Three Dominant n=1 Modes in DIII-D Experiments

Multi-pole transfer function at 3D sensor is extracted in DIII-D experiments (Shot No. 170195-170220):

$$P_j(f,\Delta\phi) = \frac{a_1^j + b_1^j e^{-i\Delta\phi}}{i2\pi f - \gamma_1} + \frac{a_2^j + b_2^j e^{-i\Delta\phi}}{i2\pi f - \gamma_2} + \frac{a_3^j + b_3^j e^{-i\Delta\phi}}{i2\pi f - \gamma_3} + c^j + d^j e^{-i\Delta\phi}\left(I_{low}/I_{up}\right),\ \Delta\phi=\phi_{low}-\phi_{up},\ \frac{I_{low}}{I_{up}} = 1$$

γ_1 = – 85.32 – 23.12i rad/s $\gamma_2 = -199.93 - 46.62i$ rad/s $\gamma_3 = -277.72 - 181.33i$ rad/s

n=1 Transfer function extracted in DIII-D experiment

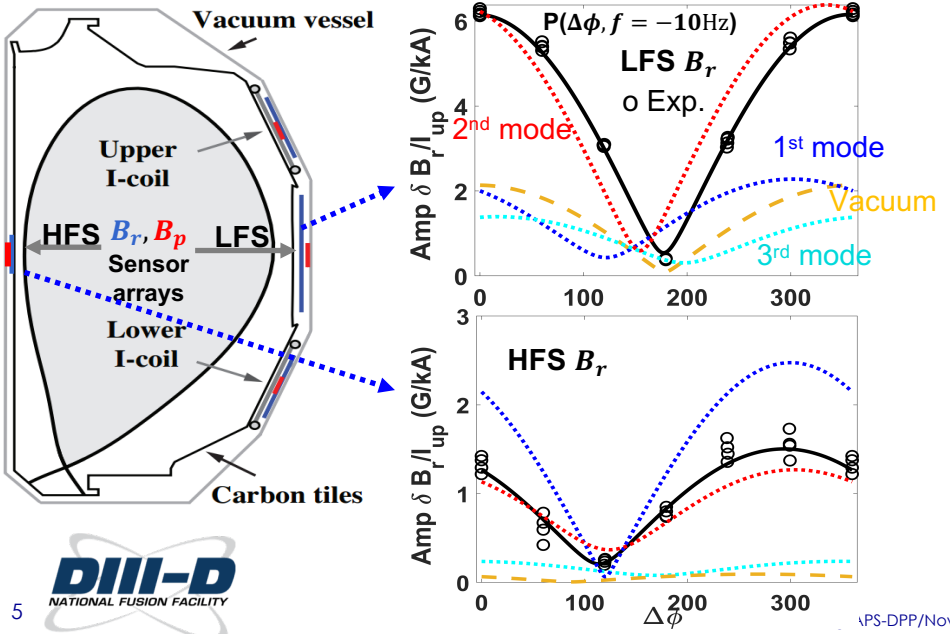

- **Plasma MHD stability can be quantified by eigenvalue of least stable mode, Re(γ_1)**
- **For any (f, $\Delta\phi$), multi-pole transfer function reveals contribution of each dominant mode at different poloidal locations of 3D sensors**

DIII-D NATIONAL FUSION FACILITY

Multi-Mode Response Analysis for EAST Experiments Identifies Two Dominant n=1 Contributions

Experimental transfer function indicates two dominant eigenmodes in EAST experiment (shot No. 70617-70633):

$$P_j(f,\Delta\phi) = \frac{a_1^j + b_1^j e^{-i\Delta\phi}}{i2\pi f - \gamma_1} + \frac{a_2^j + b_2^j e^{-i\Delta\phi}}{i2\pi f - \gamma_2} + c^j + d^j e^{-i\Delta\phi}\left(I_{low}/I_{up}\right),\ \Delta\phi=\phi_{low}-\phi_{up},\ \frac{I_{low}}{I_{up}} = 1$$

$\gamma_1 = -66.65 + 0.06i$ rad/s $\gamma_2 = -917.35 - 108.19i$ rad/s

n=1 Transfer function extracted in EAST experiment

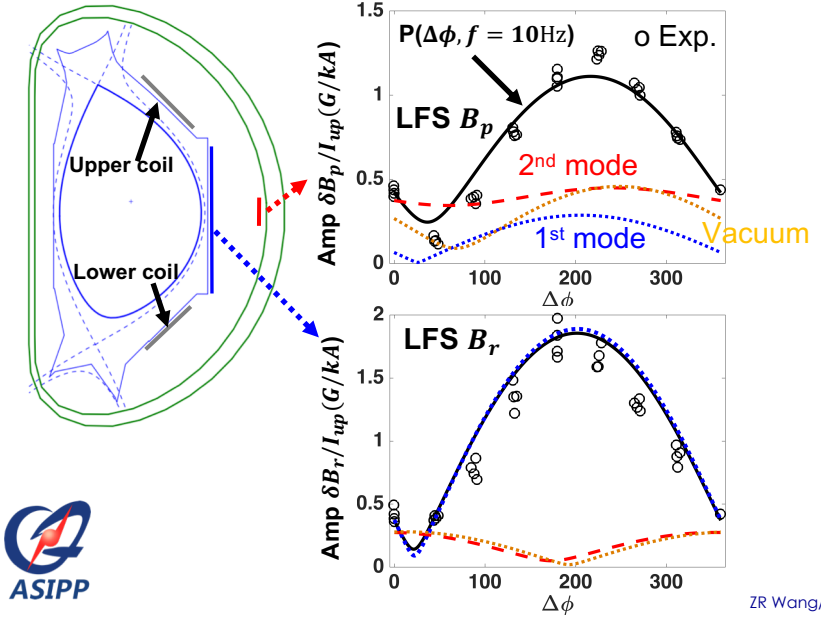

Advantage of $P(\Delta\phi, f)$ to extract stable MHD modes:

- **Inclusion of phase dependence**
  - Reduce requirement of noisy high frequency scan in conventional Nyquist method [Reimerdes et al, PRL 2004]
  - Better chance to observe significant eigenmode response
- **Extract transfer functions from multiple locations of 3D sensors simultaneously**
  - Strong constrains on eigenvalue γ_i and compensate for potential measurement errors
  - Observe more aspects of eigenmode

Outline

- Theory of multi-mode plasma response model
- Detection of n=1 modes in stable DIII-D plasma
- Multi-mode plasma response model helps to understand n=2 mode locking in L-mode DIII-D plasma

Outline

- **Theory of multi-mode plasma response model**
- Detection of n=1 modes in stable DIII-D plasma
- Multi-mode plasma response model helps to understand n=2 mode locking in L-mode DIII-D plasma

Multi-Mode Plasma Response Model is Systematically Derived From Generic Linear MHD Formulation

Linearized MHD equations including non-ideal effects

Any perturbations have form

$$x(\psi,\theta,\phi) = x^m(\psi)e^{\gamma t+im\theta+in\phi}$$

$\partial/\partial t \rightarrow \gamma$ eigenvalue

$$\gamma\vec{\xi} = -in\Omega\vec{\xi} + \vec{v} + (\vec{\xi}\cdot\nabla\Omega)R^2\nabla\phi$$

$$\gamma\vec{v} = -in\Omega\vec{v} - \rho^{-1}\nabla\cdot[\vec{\xi}\cdot\nabla P_0\vec{I} + p_{\parallel}\vec{b}\vec{b} + p_{\perp}(\vec{I}-\vec{b}\vec{b})] + \rho^{-1}(\nabla\times\vec{b})\times\vec{B}_0 + \rho^{-1}\vec{J}_0\times\vec{b} + [2\Omega\hat{Z}\times\vec{v} - (\vec{v}\cdot\nabla\Omega)R^2\vec{\nabla}\phi] - \rho^{-1}\nabla\cdot(\rho\vec{\xi})\Omega\hat{Z}\times\vec{V}_0$$

$$\gamma\vec{b} = -in\Omega\vec{b} + \nabla\times(\vec{v}\times\vec{B}_0) + (\nabla\times\vec{b}\cdot\nabla\Omega)R^2\nabla\phi - \nabla\times(\eta\nabla\times\vec{b})$$ Resistive term

Resistive wall

$$\gamma b^{\psi} = \frac{d}{\tau_w}\left(|\nabla\psi|\Delta\frac{\partial b^{\psi}}{\partial\psi} - \Delta b^{\theta}\frac{|\nabla\psi|}{\partial\theta}\right)$$

$b^1 = \vec{b}\cdot\nabla\psi$, Δ ~ wall jump

Vacuum

$$\nabla\times\vec{b} = 0 \qquad \nabla\cdot\vec{b} = 0$$

Kinetic pressure $p_{\parallel}$ and $p_{\perp}$

$$p_{\parallel}e^{-i\omega t+in\phi} = \sum_{e,i}\int d\Gamma M v_{\parallel}^2 f_L^1 \qquad p_{\perp}e^{-i\omega t+in\phi} = \sum_{e,i}\int d\Gamma\frac{1}{2}M v_{\perp}^2 f_L^1$$

Y.Q. Liu et al, PoP 2008

Discretization of computation domain

$$\vec{X}(\psi,\theta) = \left(\vec{\xi}(\psi,\theta),\vec{v}(\psi,\theta),\vec{b}(\psi,\theta)\right)^T$$

Only in plasma domain

Discretize ψ direction

Fourier transformation of θ (poloidal direction)

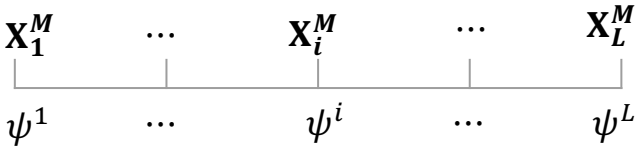

$$X_{N\times 1} = \left(X_1^M,\cdots,X_i^M,\cdots,X_L^M\right)^T \qquad X_i^M = \left(\vec{\xi}_i^M,\vec{v}_i^M,\vec{b}_i^M\right)^T$$

DIII-D NATIONAL FUSION FACILITY

Multi-Mode Plasma Response Model is Systematically Derived From Generic Linear MHD Formulation

Matrix form of equations

$$\mathbf{X}_{N\times 1} = \left(\mathbf{X}_1^M, \cdots, \mathbf{X}_i^M, \cdots, \mathbf{X}_L^M\right)^T$$

plasma / vacuum / wall / vacuum

$$\begin{pmatrix} \mathbf{I} & & \\ & \boldsymbol{\gamma}\begin{pmatrix} \mathbf{0} & \mathbf{I} \\ \mathbf{I} & \mathbf{0} \end{pmatrix} & \\ & & \end{pmatrix} \begin{pmatrix} \mathbf{X_p} \\ \mathbf{X_V^I} \\ \mathbf{X_w} \\ \mathbf{X_V^{II}} \end{pmatrix} = \begin{pmatrix} \mathbf{L_P} & \mathbf{L_{PI}} & & \\ \mathbf{L_{IP}} & \mathbf{L_I} & \mathbf{L_{IW}} & \\ & \mathbf{L_{WI}} & \mathbf{L_W} & \mathbf{L_{WII}} \\ & & \mathbf{L_{IIW}} & \mathbf{L_{II}} \end{pmatrix} \begin{pmatrix} \mathbf{X_p} \\ \mathbf{X_V^I} \\ \mathbf{X_w} \\ \mathbf{X_V^{II}} \end{pmatrix}$$

Vacuum transformation between two surfaces

$$\vec{b}_{s1}^{M} = \mathbf{T}\vec{b}_{s2}^{M}$$

Reduce vacuum equations

$\mathbf{A}$: $N\times N$ full rank matrix

$$\gamma\mathbf{IX} = \mathbf{AX}$$

$$\mathbf{A} = \mathbf{Q}\boldsymbol{\Lambda}\mathbf{Q}^{-1}$$

Eigenvalue matrix

$$\boldsymbol{\Lambda} = \begin{pmatrix} \gamma_1 & & \\ & \ddots & \\ & & \gamma_N \end{pmatrix}_{N\times N}$$

3D Coil equations and inhomogeneous plasma response equations

$$\gamma\mathbf{IX} = \mathbf{Q}\boldsymbol{\Lambda}\mathbf{Q}^{-1}\mathbf{X}$$

Upper and lower coils

$$\nabla\times\vec{\mathbf{b}} = \vec{\mathbf{j}}_{coil} \qquad \nabla\cdot\vec{\mathbf{j}}_{coil} = 0$$

coil frequency

$$\gamma = i\omega = i2\pi f$$

$$\mathbf{J}_{N\times 1}^{up}\mathrm{I}_{\mathbf{up}}e^{i\phi_{up}},\ \mathbf{J}_{N\times 1}^{low}\mathrm{I}_{low}e^{i\phi_{low}}$$

$$\mathbf{Q}(i\omega\mathbf{I}-\boldsymbol{\Lambda})\mathbf{Q}^{-1}\mathbf{X} = \mathbf{J}^{up}\mathrm{I}_{\mathbf{up}}e^{i\phi_{up}} + \mathbf{J}^{low}\mathrm{I}_{low}e^{i\phi_{low}}$$

$$\mathbf{X} = \mathbf{Q}^{-1}(i\omega\mathbf{I}-\boldsymbol{\Lambda})^{-1}\mathbf{Q}(\mathbf{J}^{up}\mathrm{I}_{\mathbf{up}}e^{i\phi_{up}} + \mathbf{J}^{low}\mathrm{I}_{\mathbf{low}}e^{i\phi_{low}})$$

$$(i\omega\mathbf{I}-\boldsymbol{\Lambda})^{-1} = \begin{pmatrix} \frac{1}{i\omega-\gamma_1} & & \\ & \ddots & \\ & & \frac{1}{i\omega-\gamma_N} \end{pmatrix}_{N\times N}$$

DIII-D NATIONAL FUSION FACILITY

Multi-Mode Plasma Response Model is Systematically Derived From Generic Linear MHD Formulation

$$\mathbf{X}_{N\times 1} = \mathbf{Q}(i\omega\mathbf{I}-\mathbf{\Lambda})^{-1}\mathbf{Q}^{-1}(\mathbf{J}^{up}\mathbf{I}_{\mathbf{up}}e^{i\phi_{up}} + \mathbf{J}^{low}\mathbf{I}_{low}e^{i\phi_{low}})$$

$\delta B = (\boldsymbol{S^1} + \boldsymbol{i\omega S^2})\boldsymbol{TX}$: sensor surface

Plasma mode - Coil coupling

$$\delta B = (\boldsymbol{R}(i\omega\mathbf{I}-\mathbf{\Lambda})^{-1} + \boldsymbol{C})(\mathbf{Q}^{-1}\mathbf{J}^{up}\mathbf{I}_{\mathbf{up}}e^{i\phi_{up}} + \mathbf{Q}^{-1}\mathbf{J}^{low}\mathbf{I}_{low}e^{i\phi_{low}})$$

Vacuum-Coil coupling $\omega \to \infty$

$\mathbf{F}^{-1}_{N\times N}$: inverse Fourier transformation

$\mathbf{M}_{1\times N}$: sensor measurement

$$\delta B = \left[(\mathbf{MF^{-1}R})_{1\times N}\begin{pmatrix}\frac{r_1}{i\omega-\gamma_1} & & \\ & \ddots & \\ & & \frac{r_N}{i\omega-\gamma_N}\end{pmatrix} + (\mathbf{MF^{-1}})_{1\times N}\begin{pmatrix}c_1 & & \\ & \ddots & \\ & & c_N\end{pmatrix}\right]\left[\begin{pmatrix}v_1^{up}\\ \vdots \\ v_N^{up}\end{pmatrix}_{N\times 1} I_{up}e^{i\phi_{up}} + \begin{pmatrix}v_1^{low}\\ \vdots \\ v_N^{low}\end{pmatrix}_{N\times 1} I_{up}e^{i\phi_{up}}\right]$$

Sensor transfer function including coil frequency $\omega = 2\pi f$ and phasing $\Delta\phi$:

Mode-Coil coupling

$$P_j(\Delta\phi, f) = \frac{\delta B}{I_{up}} = \sum_{i=1}^{N}\frac{a_i^j + b_i^j e^{-i\Delta\phi}(I_{low}/I_{up})}{i2\pi f - \gamma_i} + c^j + d^j e^{-i\Delta\phi}(I_{low}/I_{up}),\quad \Delta\phi = \phi_{low} - \phi_{up}$$

mode eigenvalue (same for each sensor)

Residual of vacuum response when $f \to \infty$

Example of $\delta\mathbf{B} = (\mathbf{S^1} + \mathbf{i\omega S^2})\mathbf{X}$

Wall equation: $\mathbf{r}[\delta\mathbf{B}_\mathbf{r}']^+_- = 2\mathbf{i\omega\tau_w\delta B_r}$

$\mathbf{\delta B_\theta \sim \delta B_r' \sim i\omega\delta B_r}$

DIII-D NATIONAL FUSION FACILITY

Proof of Principle Based on Simulated Response Data: Constructed Transfer Function Using Low-Frequency Data Recovers High-Frequency Data

- **MARS-F solves linearized ideal MHD for plasma response and eigenvalue problem**
- **MARS-F simulates n=1 DIII-D plasma response by scanning**

  $\Delta\phi$ = [0deg, 60deg, 120deg, 180deg, 240deg, 300deg]

  f= [-110Hz, -60Hz, -30Hz, -10Hz, 10Hz, 30Hz, 60Hz, 110Hz]

- **Transfer function fits MARS-F simulated data points well**
- **P($\Delta\phi, f$) agrees with Nyquist plot which is simulated by MARS-F by scanning frequency up to 10^5Hz**

MARS-F simulation of n=1 DIII-D plasma response
$q_0 = 1.03$, $q_{95} = 3.06$, $\beta_N = 1.73$

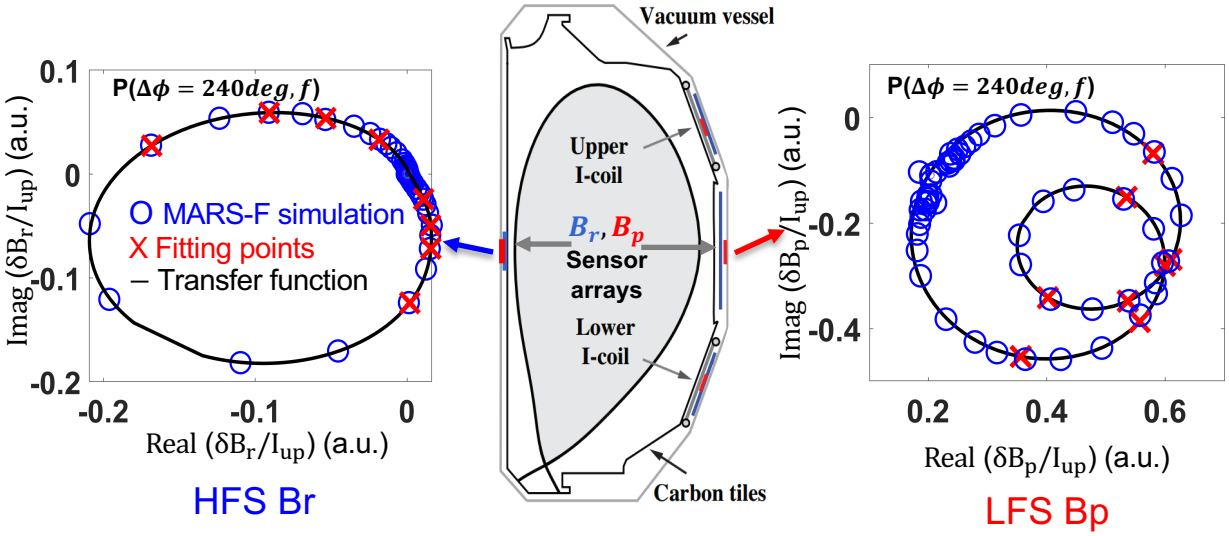

Multi-Pole Transfer Functions can be obtained from both Experimental and Numerical Data

Multi-pole transfer function on 3D sensors is developed from generalized linear-MHD theory:

$$P_j(\Delta\phi, f) = \frac{\delta B}{I_{up}} = \sum_{i=1}^{N} \frac{a_i^j + b_i^j e^{-i\Delta\phi}(I_{low}/I_{up})}{i2\pi f - \gamma_i} + c^j + d^j e^{-i\Delta\phi}(I_{low}/I_{up}), \quad \Delta\phi = \phi_{low} - \phi_{up}$$

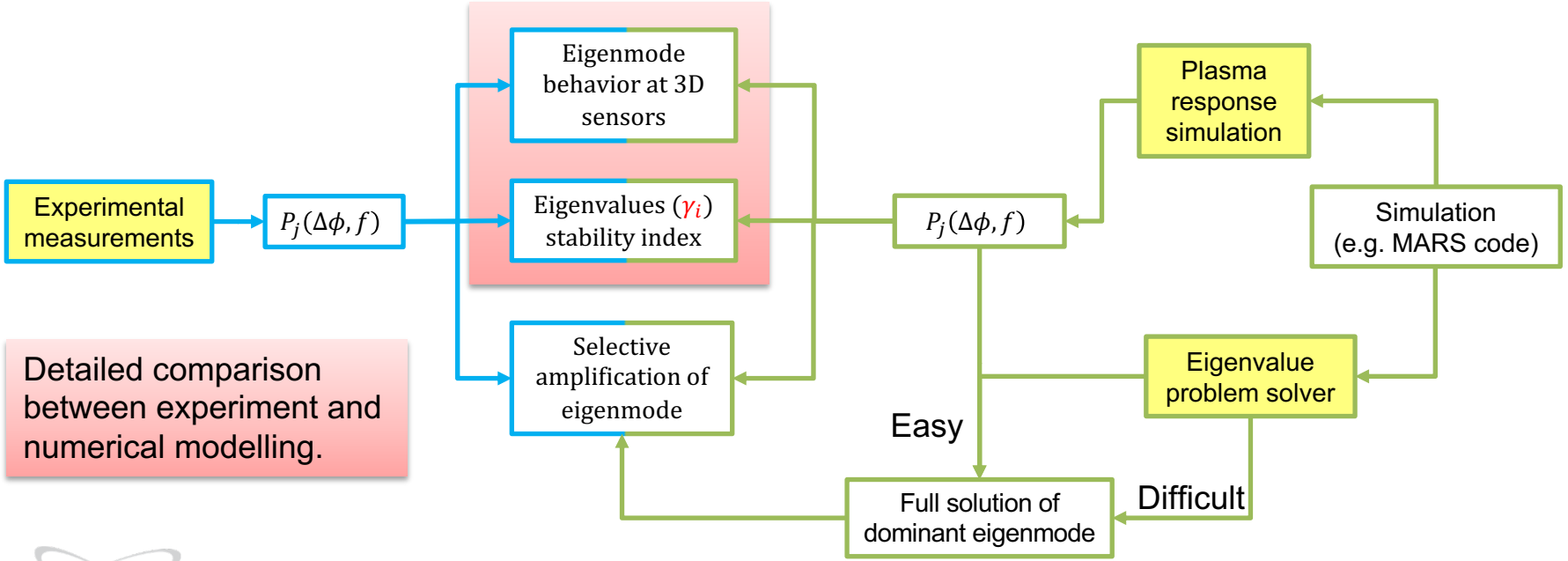

DIII-D NATIONAL FUSION FACILITY

Outline

- Theory of multi-mode plasma response model
- **Detection of n=1 modes in stable DIII-D plasma**
- Multi-mode plasma response model helps to understand n=2 mode locking in L-mode DIII-D plasma

Combined 3D MHD Spectroscopy: Scanning both Coil Phasing and Frequency to Extract Multi-Pole Transfer Function from DIII-D Experiments

- **Keep equilibrium parameters stable with little change.**
- **Repeat same discharge and scan coil phasing and frequency to measure n=1 plasma response.**
  - Change coil phasing in each discharge [170200 (0 deg), 170202 (60 deg), 170203 (120 deg), 170204 (180 deg), 170205 (240 deg),170220 (300 deg)]
  - Randomly scan coil frequency ± 10 Hz, ± 30 Hz, ± 60 Hz and ± 110 Hz in each shot
- **Frequency scan: one time interval – one frequency with several periods**

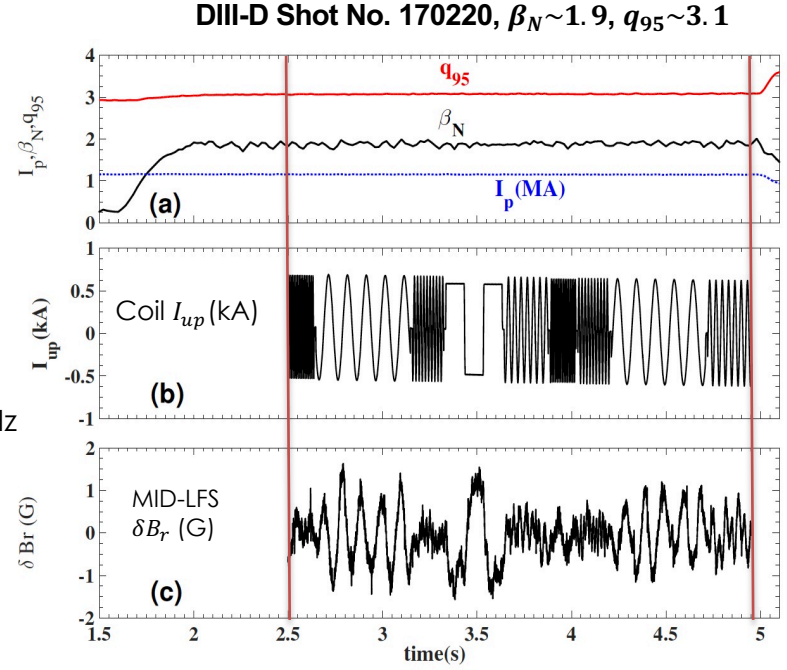

- **Extracted response at 3D sensor (Mid-LFS: δB_r, δB_p; Mid-HFS: δB_r, δB_p):**

$$\delta B = Ae^{i(2\pi ft+\phi-n\phi_{tor})}$$

DIII-D NATIONAL FUSION FACILITY

Combined 3D MHD Spectroscopy: Response Extracted by Simultaneous Fitting of DIII-D Data from Multiple Sensors

Multi-pole response transfer functions fit to multiple sensor measurements at Mid-HFS (B_r and B_p) and Mid-LFS (B_r and B_p)

$$P_j(\Delta\phi, f) = \frac{\delta B}{I_{up}} = \sum_{i=1}^{N} \frac{a_i^j + b_i^j e^{-i\Delta\phi}(I_{low}/I_{up})}{2\pi i f - \gamma_i} + c^j + d^j e^{-i\Delta\phi}(I_{low}/I_{up})$$

Nonlinear least square fitting is used to find γ_i, a_i and b_i by minimizing target function:

$$\min\left\{\sum\left|\frac{\delta\hat{B}^{exp} - P_j}{\delta\hat{B}^{exp}}\right|^2\right\}, \qquad \delta\hat{B}^{exp} = \frac{\delta B^{exp}}{I_{up}}$$

Three stable dominant modes are extracted:

$\gamma_1 = -85.32 - 23.12i$ rad/s
$\gamma_2 = -199.93 - 46.62i$ rad/s
$\gamma_3 = -277.72 - 181.33i$ rad/s

Qualitative index of MHD modes' stabilities

Convergence test of transfer function:

- **Randomly perturbing initial guess**
- **Increase pole number during fitting**

  Contribution of 4th and 5th modes is negligible

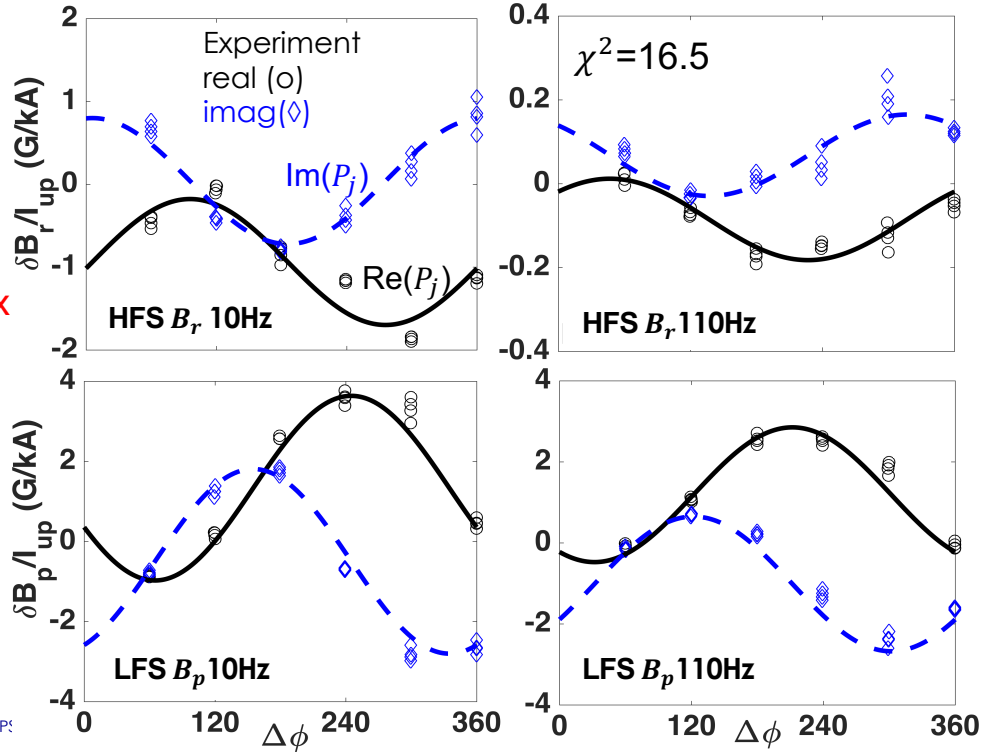

DIII-D NATIONAL FUSION FACILITY

Construction of Transfer Functions from Both Measured and Simulated Response Data Allows Direct Comparison of Each Individual Mode

- **Transfer function can be extracted from MARS-F simulation by performing same phasing and frequency scan as experiments**
- **Each dominant eigenmode can be compared separately between experiments and simulations**

General behavior of each mode is similar between experiment and simulation

Experiment	MARS-F
γ_1 = –85.32 – 23.12i rad/s	–45.18 – 2.95i rad/s
γ_2 = −199.93 − 46.62i rad/s	–101.22 – 0.75i rad/s
γ_3 = −277.72 − 181.33i rad/s	–365.99+ 3.39i rad/s

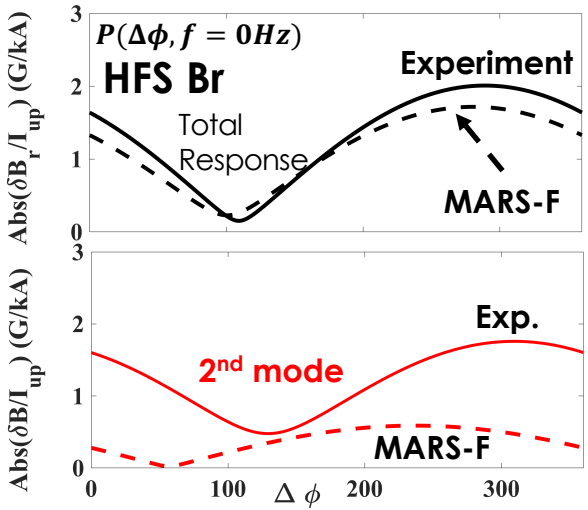

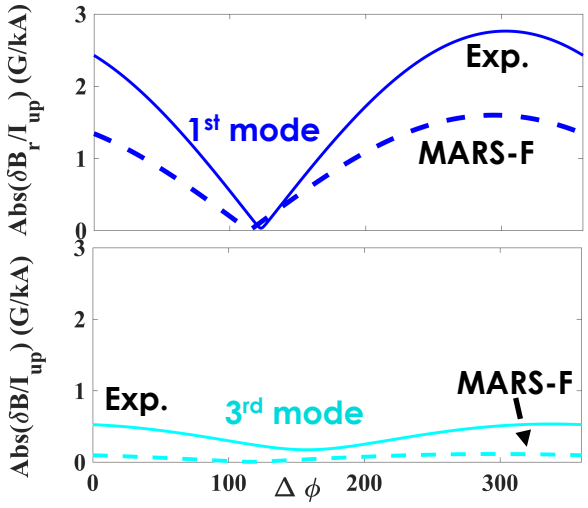

DIII-D NATIONAL FUSION FACILITY

Reconstructed Stable Poles Are Used to Guide Eigenvalue Solver to Directly Compute Eigenmode Structure for 3 Dominant Modes

- **Eigenvalues from simulated transfer function, as initial guess of eigenvalue problem solved by MARS-F , help to find converged solutions.**
- **Different eigenmode structure has potential for different application purpose.**

  1st mode: core rotation control through NTV torque

  3rd mode: help edge island open for ELM suppression

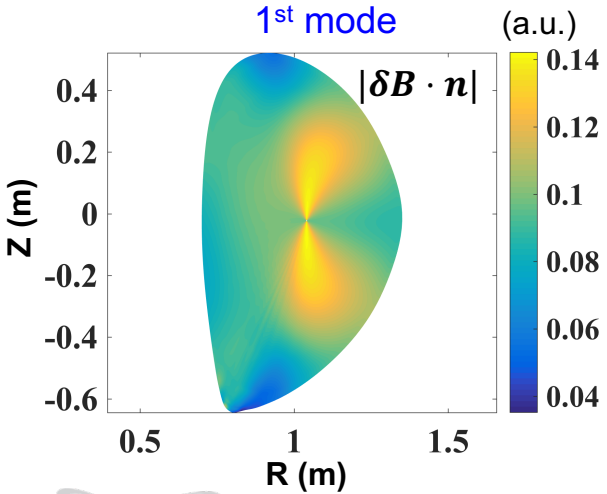

Core dominant

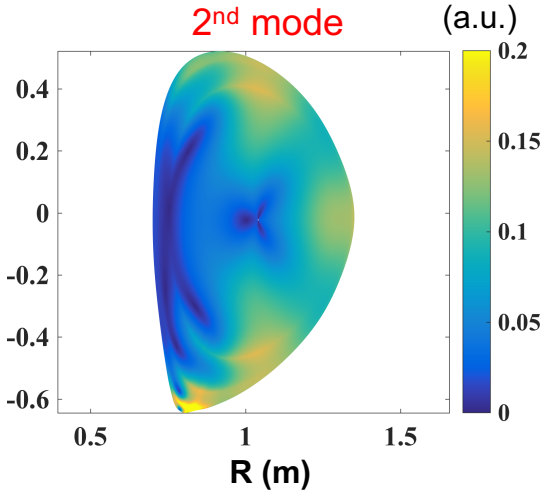

Divertor dominant

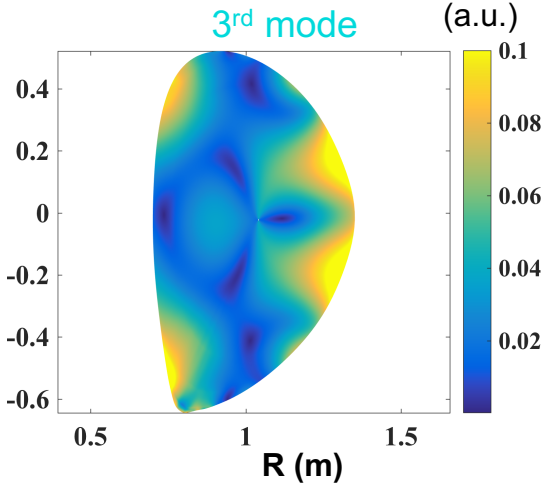

Edge dominant

DIII-D NATIONAL FUSION FACILITY

Transfer Function Reconstructed From Experimental Data Helps to Perform Selective Amplification of Mode in 2D Space of Coil Phasing and Frequency

- Phasing and frequency dependence of each dominant eigenmode can be evaluated by transfer function
- 2D scan of coil frequency and phasing could help to amplify preferred eigenmode.
- Higher coil frequency makes stronger amplification of 2nd and 3rd modes in concerned DIII-D experiment

$(\Delta\phi, f)$ dependence of mode amplitude at HFS δB_r

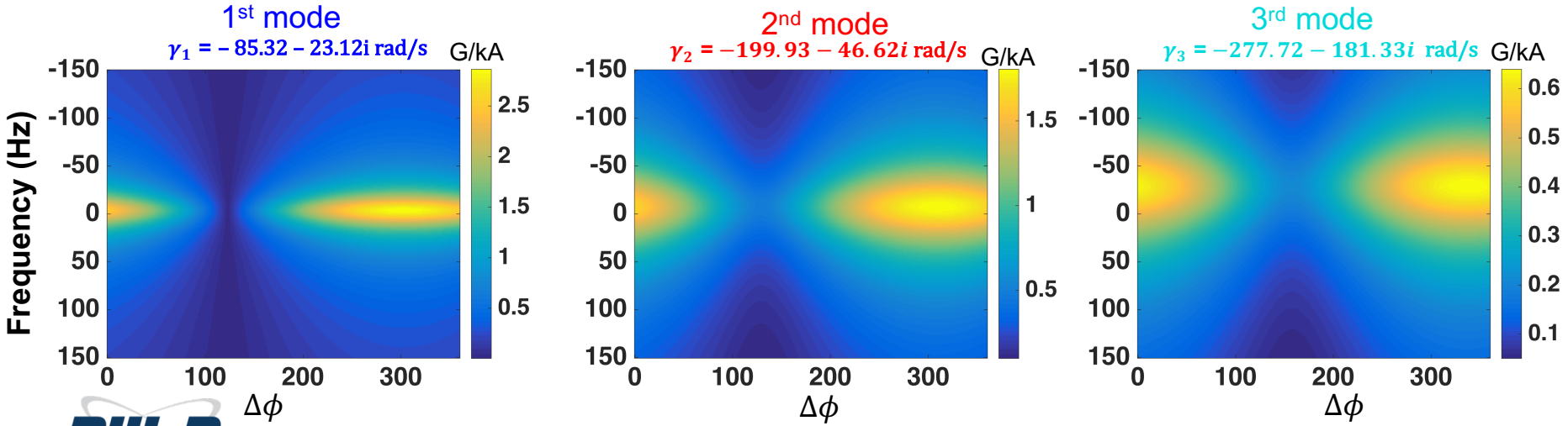

DIII-D NATIONAL FUSION FACILITY

Transfer Function Reconstructed From Experimental Data Helps to Perform Selective Amplification of Mode in 2D Space of Coil Phasing and Frequency

- Phasing and frequency dependence of each dominant eigenmode can be evaluated by transfer function
- 2D scan of coil frequency and phasing could help to amplify preferred eigenmode.
- Higher coil frequency makes stronger amplification of 2nd and 3rd modes in concerned DIII-D experiment

$(\Delta\phi, f)$ dependence of mode amplitude at HFS δB_r

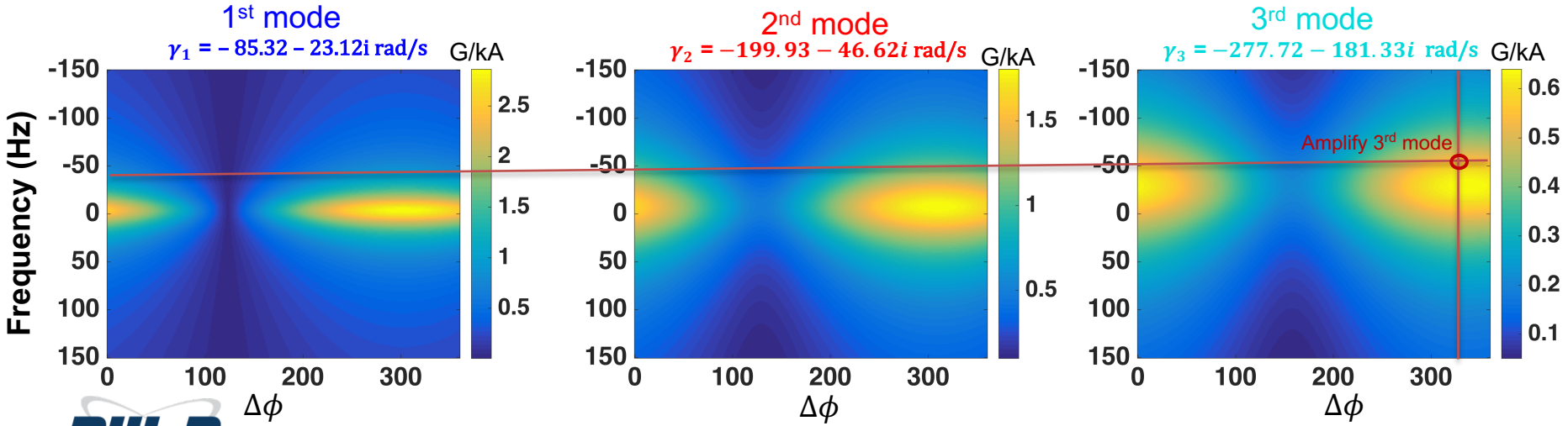

DIII-D NATIONAL FUSION FACILITY

Outline

- Theory of multi-mode plasma response model
- Detection of n=1 modes in stable DIII-D plasma
- **Multi-mode plasma response model helps to understand n=2 mode locking in L-mode DIII-D plasma**

More Efficient MHD Spectroscopy with Multi-Frequency Wave Package Applied in DIII-D L-Mode for n=2 Mode Identification

- **Efficiency of coil phasing and frequency scan is improved by applying multiple frequencies simultaneously .**

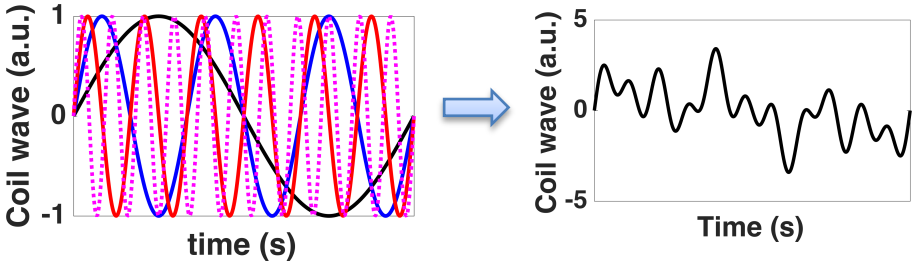

Wave packet for given phasing (0°, 90°, 180°, 270°) is carefully designed by combining multiple waves ($\pm 10Hz$, $\pm 30Hz$, $\pm 60Hz$, $\pm 110Hz$).

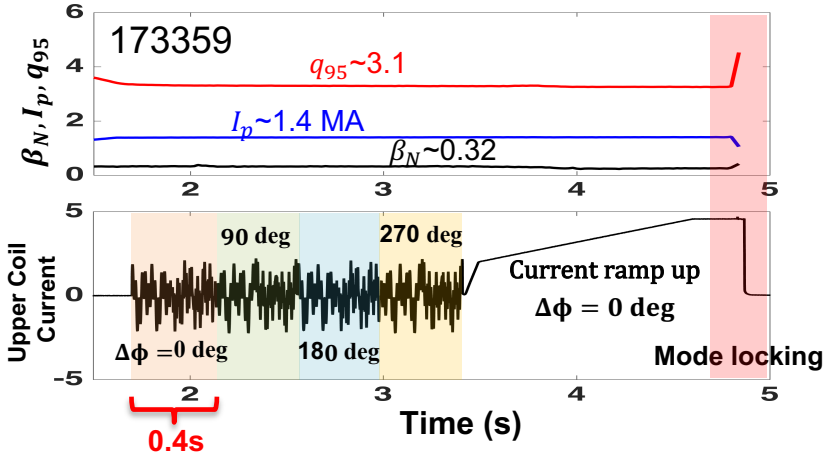

- **Two dominant modes are extracted from experiments**

$\gamma_1 = -212.81 + 23.81i$ rad/s
$\gamma_2 = -327.23 - 142.63i$ rad/s

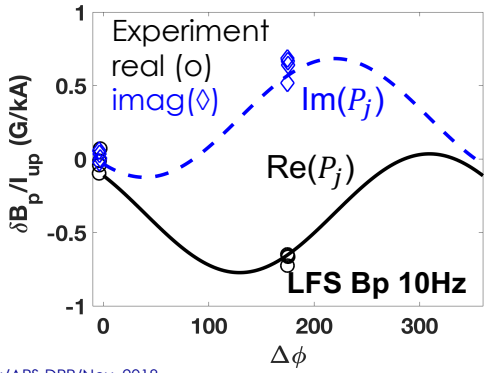

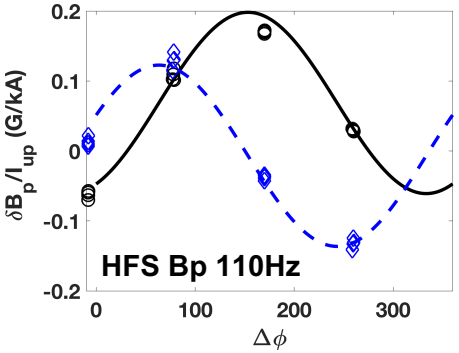

DIII-D NATIONAL FUSION FACILITY

n=2 Combined MHD Spectroscopy Identifies Least Stable Mode as Stable Tearing Mode and Confirmed by MARS-F Eigenvalue Computation

Mode comparison between Expt. and Simulation

Experiment	MARS-F
$\gamma_1 = -212.81 + 23.81i$ rad/s	$-205.46 - 7.29i$ rad/s
$\gamma_2 = -327.23 - 142.63i$ rad/s	$-1.66\times10^3 - 15.02i$ rad/s

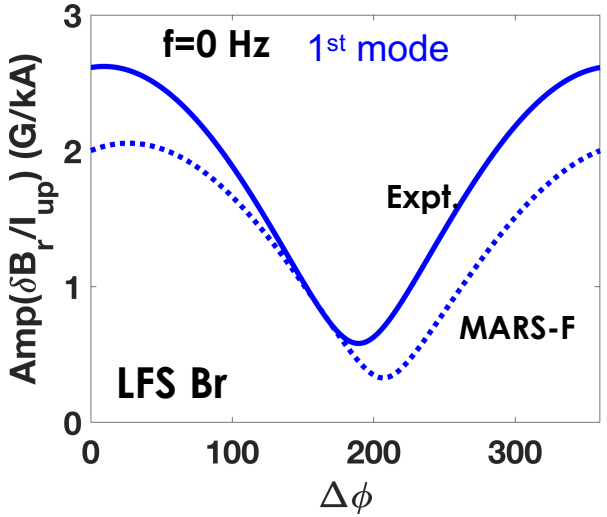

- 1st mode computed by MARS-F similar to that extracted from experiment
- MARS-F eigenvalue runs scanning plasma resistivity ➔ 1st mode corresponds to an unstable TM at high resistivity

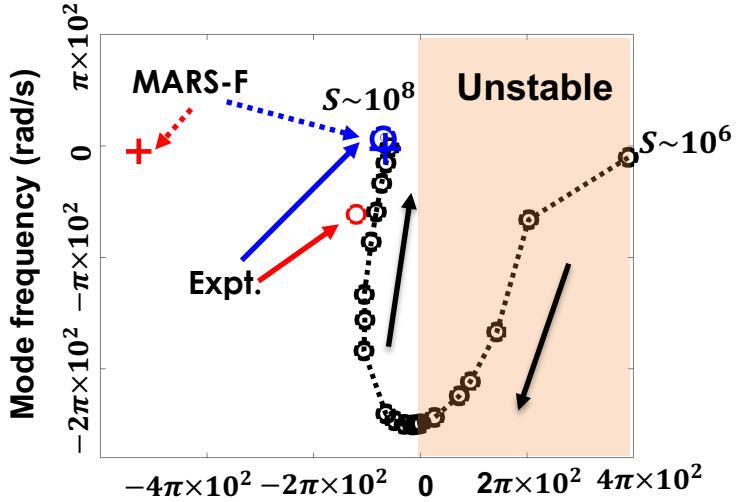

S: Lundquist number

Liu et al, PoP 2012

Amplification of Stable Tearing Component at $\Delta\phi$=0° ➔ Strong Resonant Perturbations ➔ Lower Mode Locking Threshold

- **MARS-F solves eigenvalue problem to find eigenmode structure of two dominant modes**
  - Least stable mode is resistive eigenmode
  - Secondary mode has global kink structure
- **n=2 Least Stable Mode is Amplified at $\Delta\phi$=0 Degree Coil Phasing (Even Parity) with Clear Tearing Structure**

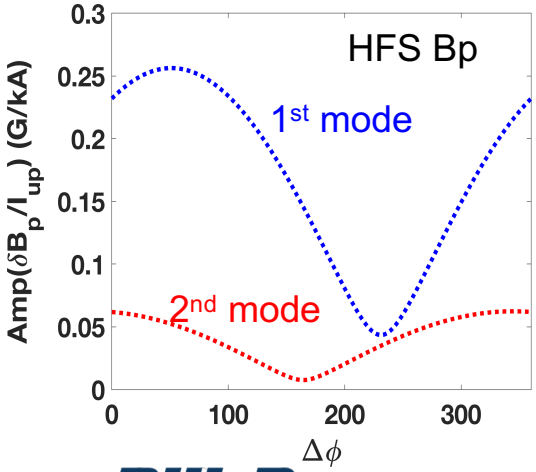

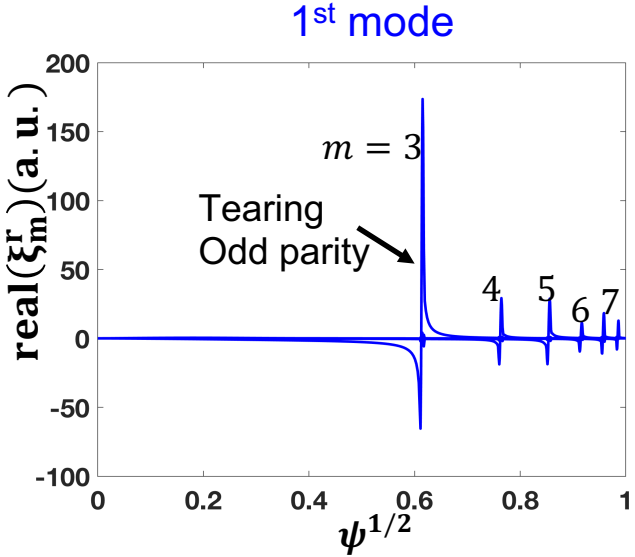

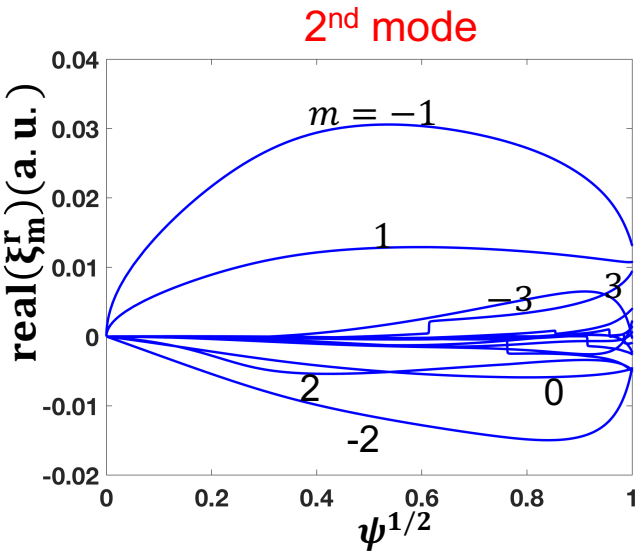

DIII-D NATIONAL FUSION FACILITY

Thesis: Multi-Mode Plasma Response Model and Combined 3D MHD Spectroscopy Provide Pertinent Tools to Study Stable MHD Modes

- **Multi-mode plasma response model/plasma transfer function developed from linear MHD and control theory can identify:**
  - Spatial structure of each dominant stable mode in multi-mode plasma response
  - Damping rates of dominant modes as quantitative index of plasma stability
- **Extraction of stable eigenmodes, using multi-mode plasma response model, is validated in tokamak experiments**
- **Comparison between experimentally extracted multi-mode response and MARS-F simulations:**
  - Identify n=2 resistive eigenmode as least stable and amplified at $\Delta\phi$=0 deg, lead to lower mode locking threshold
- **Multi-mode plasma response model is a powerful tool for**
  - Optimizing RMP spectrum to amplify preferred eigenmode for ELM suppression
  - Real-time quantitative monitoring plasma stability

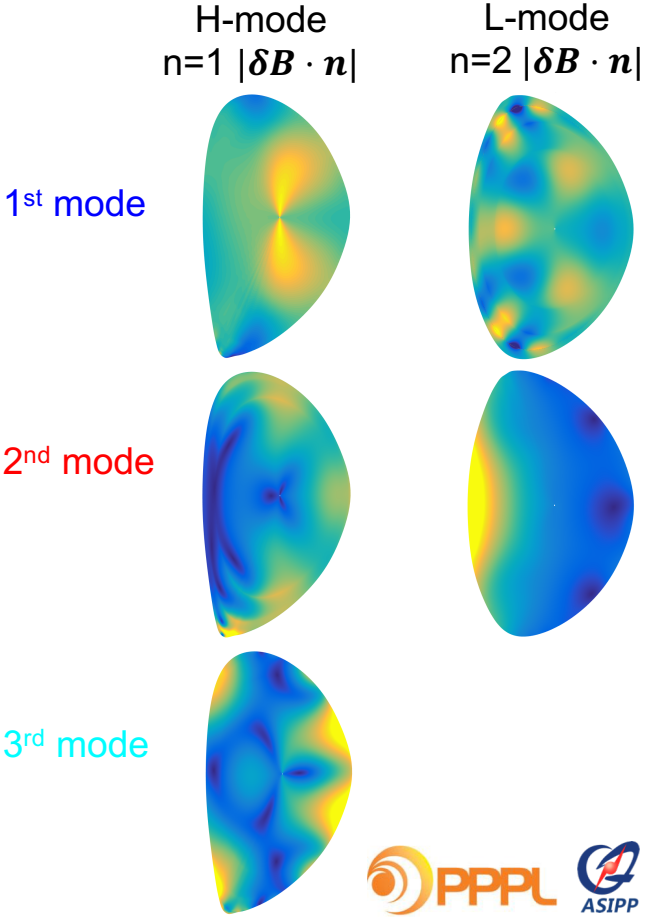

DIII-D NATIONAL FUSION FACILITY

PPPL ASIPP

Backup slides

Experimental Extracted Plasma Response Model is Verified with Independent Experiment

- **Experiment (shot No. 170196)** only uses upper I-coil to scan frequency
- Transfer function, extracted from phasing and frequency scan of I-coils, shows good agreement with sensor measurements in independent experiment
- Experiment confirms linear approach of plasma response in theory

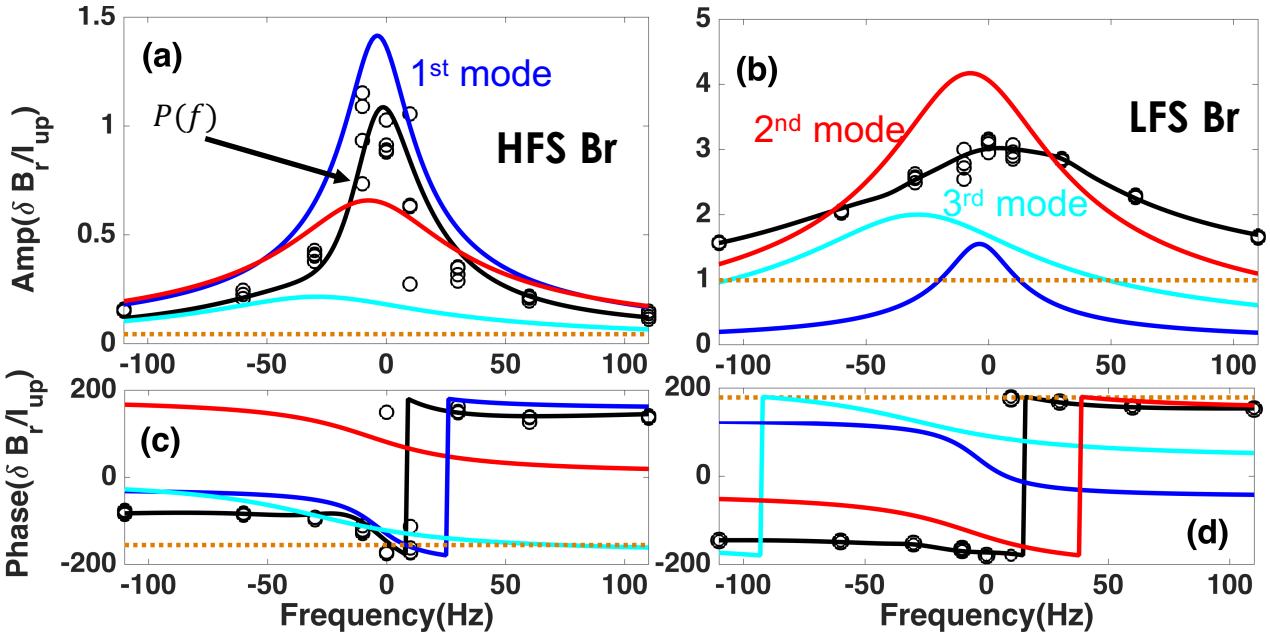

DIII-D NATIONAL FUSION FACILITY

Multi-Mode Response Transfer Function Reveals Contribution of Each Eigenmode While Applying Different Coil Frequency and Phasing

This slides maybe not shown in talk

Eigenvalue of three dominant modes:

$\gamma_1 = -10.96 + 1.23i$ Hz
$\gamma_2 = -112\times10^2 - 14.93i$ Hz
$\gamma_3 = -1.45\times10^2 - 2.32\times10^2 i$ Hz

- **Contribution of each dominant mode can be separated at any frequency and phasing**
- **$\Delta\phi$=100 deg has least stable mode dominant. $\Delta\phi$=240deg makes 2nd and 3rd modes more important**

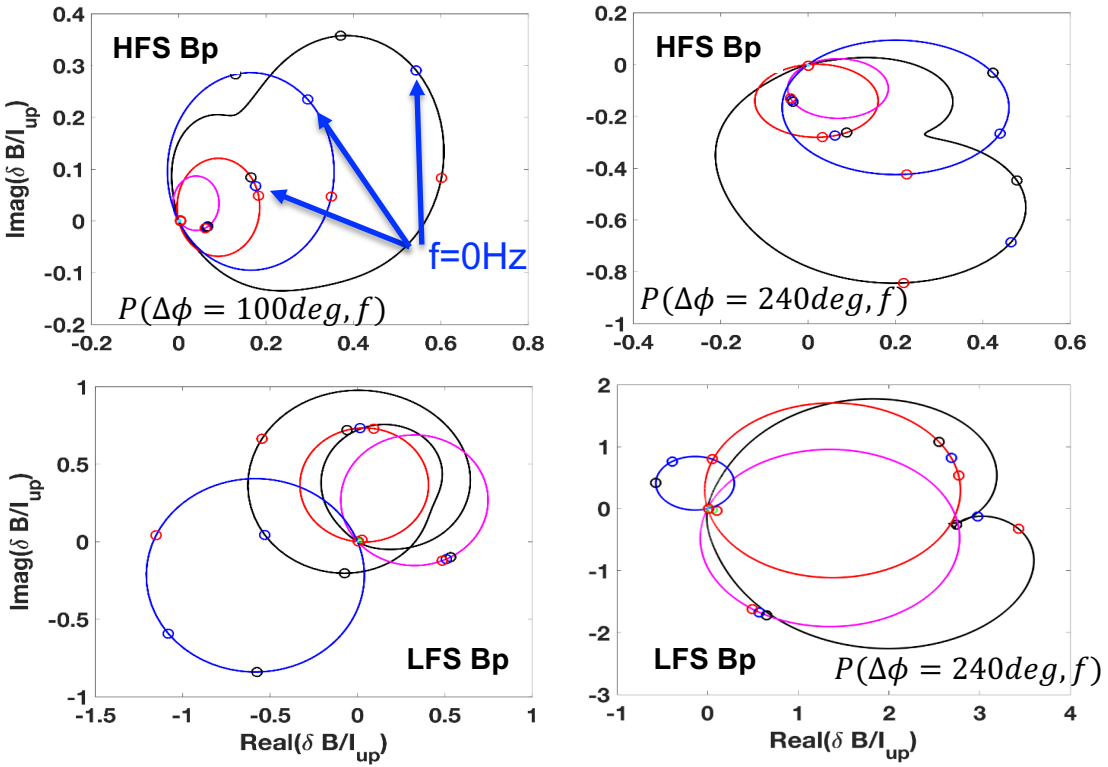

DIII-D NATIONAL FUSION FACILITY

Resistive Wall Effect is Important to Determine Plasma Response While Rotating 3D Fields are Applied.

- In coil frequency scan, simulated LFS δB_r with different wall time decays faster than experimental transfer function.
- An sophisticated wall modelling is important to AC plasma response simulation.

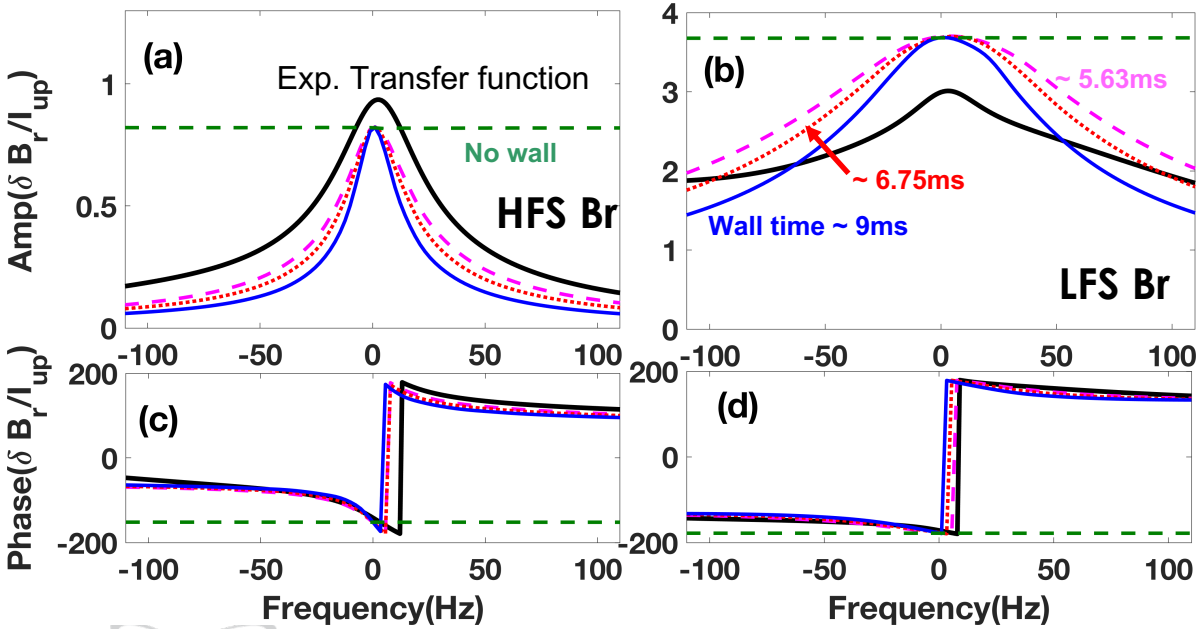

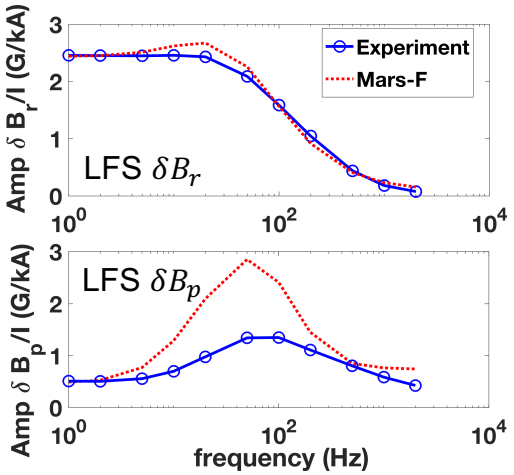

2D wall with uniform resistivity is not sufficient to resolve spatial details of wall eddy current patterns to simulate local magnetic measurements.

J.M. Hanson et al, Nucl. Fusion 2016

DIII-D NATIONAL FUSION FACILITY

Well Restore Magnetic Response in Time Domain

HFS Br, $\Delta\phi = 240\ deg$

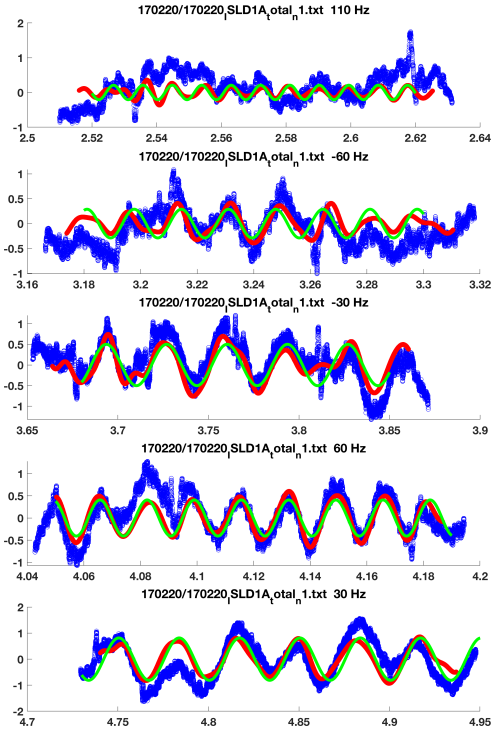

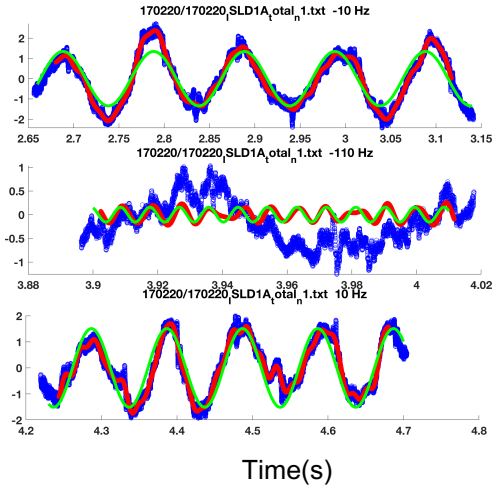

Raw data

Band pass filter

Transfer function

DIII-D NATIONAL FUSION FACILITY

Single Mode Response Also Leads to Different $\Delta\phi$ of Minimum Amplitude at LFS and HFS (Toy model)

Consider two driving terms $\boldsymbol{I^{up}}e^{i\phi_{up}}$ and $\boldsymbol{I^{low}}e^{i\phi_{low}}$, response measured by sensor at θ_s:

$$R^s = \frac{[a_1^{up}(\theta_s) + a_1^{low}((\theta_s))e^{i(\phi_{low}-\phi_{up})}]\boldsymbol{v_1}(\boldsymbol{\theta})e^{i\phi_{up}}}{\lambda_1}$$

$$a_1^{up}(\theta_s) = \left|a_1^{up}(\theta_s)\right|e^{i\phi_1^{up}(\theta_s)} \qquad a_1^{low}(\theta_s) = \left|a_1^{low}(\theta_s)\right|e^{i\phi_1^{low}(\theta_s)}$$

$$|R^s| = \frac{|\boldsymbol{v_1}(\boldsymbol{\theta})|}{|\lambda_1|}\left||a_1^{up}(\theta_s)| + |a_1^{low}((\theta_s))|e^{-i[\underbrace{(\phi_{up}-\phi_{low})}_{\Delta\phi}-\underbrace{(\phi_1^{low}(\theta_s)-\phi_1^{up}(\theta_s))}_{\Delta\phi_{sen}(\theta_s)}]}\right|$$

$$\Delta\phi = \Delta\phi_{sen}(\theta_s) \pm \pi \Longrightarrow |R^s|_{min}$$

θ_s dependence of $|R^s|_{min}$ even for single mode

Single Mode Response Also Leads to Different $\Delta\phi$ of Minimum Amplitude at LFS and HFS (Toy model)

Consider a complex linear system: $\boldsymbol{A(\theta)}x = 0$

$\boldsymbol{v(\theta)\Lambda v^{-1}(\theta)}x = 0$

→ Eigen functions (span solution space): $\boldsymbol{v}_1(\theta), \boldsymbol{v}_2(\theta), \ldots, \boldsymbol{v}_n(\theta)$

→ Eigen values: $\lambda_1, \lambda_2, \ldots, \lambda_n$

Response to a driving term: $\boldsymbol{A(\theta)}x = \boldsymbol{I}$

$\boldsymbol{v(\theta)\Lambda v^{-1}(\theta)}x = \boldsymbol{I}$

→ Multi-mode solution: $x(\theta) = \frac{i_1(\theta)}{\lambda_1}\boldsymbol{v}_1(\theta) + \frac{i_2(\theta)}{\lambda_2}\boldsymbol{v}_2(\theta) + \cdots + \frac{i_n(\theta)}{\lambda_n}\boldsymbol{v}_n(\theta)$

If only one mode, single-mode solution: $x(\theta) = \frac{i_1(\theta)}{\lambda_1}\boldsymbol{v}_1(\theta)$

Response measured by sensor S : $R = Sx(\theta) = \frac{Si_1(\theta)}{\lambda_1}\boldsymbol{v}_1(\theta)$

Here, $i_1(\theta)$, $i_2(\theta)$,…, $i_n(\theta)$ are complex coupling coefficients of coil current to each mode.

Consider two driving terms $\boldsymbol{I^{up}}e^{\phi_{up}}$ *and* $\boldsymbol{I^{low}}e^{\phi_{low}}$, response measured by sensor S^{LFS} and S^{HFS} at mid-plane of LFS ($\theta = 0$) and HFS ($\theta = \pi$) respectively

$$R^{LFS} = \frac{S^{LFS}[i_1^{up}(0) + i_1^{low}(0)e^{i(\phi_{low}-\phi_{up})}]\boldsymbol{v_1(\theta)}e^{i\phi_{up}}}{\lambda_1}$$

$$R^{HFS} = \frac{S^{HFS}e^{im\pi}[i_1^{up}(\pi) + i_1^{low}(\pi)e^{i(\phi_{low}-\phi_{up})}]\boldsymbol{v_1(\pi)}e^{i\phi_{up}}}{\lambda_1}$$

The minimum point is determined by $\phi_{min}(0) = ang(i_1^{up}(0)) - ang(i_1^{low}(0)) \pm \pi$ and $\phi_{min}(\pi) = ang(i_1^{up}(\pi)) - ang(i_1^{low}(\pi)) \pm \pi$.

Here, single mode is amplified by upper and lower coils respectively. It can have $i_1^{up}(0) \neq i_1^{low}(0)$ and $i_1^{up}(\pi) \neq i_1^{low}(\pi)$.

At LFS and HFS, the coupling between mode and coil can be different, $i_1^{up}(0) \neq i_1^{up}(\pi)$ and $i_1^{low}(0) \neq i_1^{low}(\pi)$. Therefore, $i_1^{up}(0) \neq i_1^{up}(\pi) \neq i_1^{low}(0) \neq i_1^{low}(\pi)$.

It is possible to have $\phi_{min}(0) \neq \phi_{min}(\pi)$.

Physical understanding: single mode is amplified twice by upper and lower coils respectively. The coupling of single mode to upper and lower coils can be different at LFS and HFS. While changing $e^{\phi_{low}-\phi_{up}}$, the combination of two amplifications can be different at LFS ($i_1^{up}(0) + i_1^{low}(0)e^{i(\phi_{low}-\phi_{up})}$) and HFS($i_1^{up}(\pi) + i_1^{low}(\pi)e^{i(\phi_{low}-\phi_{up})}$).